EDGE ARTICLE

Structural re-arrangement in two hexanuclear Cu^II complexes: from a spin frustrated trigonal prism to a strongly coupled antiferromagnetic soluble ring complex with a porous tubular structure†

Walter Cañon-Mancisidor,[ab] Carlos J. Gómez-García,*[c] Guillermo Mínguez Espallargas,*[c] Andres Vega,[bd] Evgenia Spodine,[ab] Diego Venegas-Yazigi[be] and Eugenio Coronado*[c]

The addition of water to a chloroform solution of the Cu_6 trigonal prism complex $[Cu_6(\mu_6F)(\mu_2OH)(\mu_3OCH_3)_2(\mu_2OCH_3)_2(3,5\text{-}Me_2pz)_6]$ (**1**) (3,5-Me_2pz^- = 3,5-dimethylpyrazolate) results in the formation of the Cu_6 planar hexagonal ring complex $[Cu_6(\mu_2OH)_6(3,5\text{-}Me_2pz)_6]\cdot CH_3CN\cdot CHCl_3$ (**2**). A simple mechanism for this structural re-arrangement is proposed, in which **2** can be viewed as a hydrolysis product of **1**. This process is clearly noticeable in the magnetic properties, which change from spin frustrated with a weak antiferromagnetic coupling in **1**, to strongly antiferromagnetic in **2**. Interestingly, the hexagonal ring complex **2** self-assembles in the solid state to form a porous hexagonal tubular structure containing guest solvent molecules that can be removed and CO_2-exchanged without loss of crystallinity.

Introduction

A recurrent topic in coordination chemistry is that of searching for new polynuclear complexes based on copper(II). In fact, thanks to its coordination plasticity and large affinity towards N-donor ligands, this ion has provided a huge variety of polynuclear structures showing different nuclearities and dimensionalities,[1,2] which have been shown to be of interest in diverse areas such as catalysis,[3] bio-inorganic chemistry,[4–7] materials chemistry[8,9] and molecular magnetism, just to name a few. In molecular magnetism, for example, polynuclear Cu^II complexes have been extensively studied as model systems to gain insight into the exchange interaction phenomenon in both discrete units and extended structures.[10]

An aspect that has been much less investigated is how the structures of these polynuclear Cu^II complexes change under the influence of a chemical stimulus. Here the coordination plasticity around Cu^II can also play a key role. For example, in the solid state there are many examples of flexible coordination polymers in which the structural changes caused by the uptake/release of physisorbed or chemisorbed molecules are facilitated by changes induced in the Cu^II coordination environment.[11,12] In solution these chemically-induced structural rearrangements are also present, although it is often difficult to isolate the different chemical species involved in the process.

Here we report the synthesis of two new hexanuclear Cu^II complexes that form crystals of formula $[Cu_6(\mu_6F)(\mu_2OH)(\mu_3OCH_3)_2(\mu_2OCH_3)_2(3,5\text{-}Me_2pz)_6]$ (**1**) and $[Cu_6(\mu_2OH)_6(3,5\text{-}Me_2pz)_6]\cdot CH_3CN\cdot CHCl_3$ (**2**), where 3,5-Me_2pz^- (3,5-dimethylpyrazolate) is a pyrazole derivative which acts as a bridging ligand. In solution, complex **1** is transformed into **2** upon addition of water. Thus, complex **1** exhibits a trigonal prismatic geometry, which transforms into a hexagonal ring geometry (complex **2**) when water is added to a $CHCl_3$ solution of **1**. Here we propose a possible hydrolysis mechanism for the transformation of **1** into **2**. We show that these structural changes have a strong influence on their magnetic properties and finally, we examine the porosity properties of crystals of **2**, which exhibit a hexagonal tubular structure that allows partial removal of the internal solvent molecules and absorption of CO_2.

[a]*Facultad de Ciencias Químicas y Farmacéuticas, Universidad de Chile, Santiago, Chile. E-mail: wcanon@ciq.uchile.cl; espodine@uchile.cl; Fax: +56 229786; Tel: +56 229782862*

[b]*CEDENNA, Chile*

[c]*Instituto de Ciencia Molecular (ICMol), Universidad de Valencia, C/ Catedrático José Beltrán, 2, 46980 Paterna, Valencia, Spain. E-mail: carlos.gomez@uv.es; eugenio.coronado@uv.es; guillermo.minguez@uv.es; Fax: +34963543273; Tel: +34963544423*

[d]*Universidad Andrés Bello, Departamento de Ciencias Químicas, Santiago, Chile. E-mail: andresvega@unab.cl*

[e]*Facultad de Química y Biología, Universidad de Santiago de Chile, USACH, Chile. E-mail: diego.venegas@usach.cl; Fax: +56 226812108; Tel: +56 227181079*

† Electronic supplementary information (ESI) available: CCDC 927862–927865. For ESI and crystallographic data in CIF or other electronic format see DOI: 10.1039/c3sc52628c

Experimental

Synthesis of the complexes

All chemicals were of reagent grade and used without further purification.

$[Cu_6(\mu_6\text{-}F)(\mu_2\text{-}OH)(\mu_3\text{-}OCH_3)_2(\mu_2\text{-}OCH_3)_2(3,5\text{-}Me_2pz)_6]$ **(1)**. 3,5-Dimethylpyrazole (288 mg, 3 mmol) and diethylamine (220 mg, 3 mmol) were dissolved in 15 mL of $CHCl_3$ and stirred for 20 minutes. This solution was added drop-wise into a solution of $Cu(BF_4)_2 \cdot H_2O$ (712 mg, 3 mmol) in 15 mL of CH_3OH. The greenish solution was stirred for 3 hours. Diethyl ether was diffused into the solution, and green crystals suitable for X-ray diffraction were obtained within one day (yield = 360 mg, 65%). This compound can also be prepared using CH_3OH instead of $CHCl_3$ to prepare the first solution. Phase purity was established by XRPD (Fig. S1†). Elemental analysis for **1**: found: C, 35.5; N, 14.6; H, 4.9%. Calc. for $C_{34}H_{55}N_{12}O_5FCu_6$: C, 36.7; N, 15.1; H, 5.0%. Elemental ratio estimated by electron probe microanalysis (EPMA): found: Cu : F = 6.0. Calc. for $C_{34}H_{55}N_{12}O_5FCu_6$: Cu : F = 6.0.

$[Cu_6(\mu_2\text{-}OH)_6(3,5\text{-}Me_2pz)_6] \cdot CH_3CN \cdot CHCl_3$ **(2)**. 5 mL of water was added with stirring to a green solution containing 637 mg (0.57 mmol) of compound **1** in 20 mL of $CHCl_3$, resulting in the separation of two phases and a colour change from green to purple in the organic phase. The two phases were separated, and the diffusion of acetonitrile into the organic phase yielded purple crystals of compound **2** suitable for X-ray diffraction within one day (yield = 284 mg, 45%). Phase purity was established by XRPD (Fig. S2†). Elemental analysis for **2**: found: C, 32.6; N, 14.6; H, 4.0%. Calc. for $C_{33}H_{52}N_{13}Cl_3O_6Cu_6$: C, 32.6; N, 15.0; H, 4.3%. The EPMA analysis ruled out the presence of any F^- in complex **2** and showed a Cu : Cl ratio of 2.0, in agreement with the proposed formula.

Single crystal X-ray diffraction

Single crystals of compounds **1** and **2** were mounted on a glass fibre using a viscous hydrocarbon oil to coat the crystal. X-ray data were collected at room temperature for **1**. A single crystal of **2** was structurally characterized at 120 K, then heated to 373 K for 6 h, after which most of the solvent molecules were removed, as shown after the structural determination (**2′-373**). The crystal was then cooled to 120 K and crystal structure determination was re-undertaken (**2′-120**). X-ray data were collected on a Supernova diffractometer equipped with a graphite-monochromated Enhance (Mo) X-ray source ($\lambda = 0.71073$ Å). The program CrysAlisPro, Oxford Diffraction Ltd., was used for unit cell determinations and data reduction. Empirical absorption correction was performed using spherical harmonics, implemented in the SCALE3 ABSPACK scaling algorithm. Crystal structures were solved and refined against all F^2 values using the SHELXTL suite of programs.[13] Non-hydrogen atoms were refined anisotropically and hydrogen atoms were placed in calculated positions that were refined using idealized geometries (riding model) and assigned fixed isotropic displacement parameters except for that of the hydroxido ligand, which was located and refined with distance restraints. In **2**, the non-coordinated solvent molecules ($CHCl_3$ and CH_3CN) are disordered over two sites (related by an inversion

centre) and have been modelled with 50 : 50 ratios. The void volumes in **2′-373** and **2′-120** were estimated using PLATON to be 16.7% and 14.7% of the unit cell, respectively. SQUEEZE[14] analysis shows that no solvent molecules are present in **2′-373**, whereas a small amount of residual electron density (8 electrons) is found in **2′-120**. This is attributed to the presence of some interstitial solvent molecules that remain in the channel, which are highly disordered at high temperature and freeze upon lowering the temperature. All efforts to model this residual electron density were unsuccessful. A summary of the data collection and structure refinements is provided in Table S1.†

Physical characterisation

Variable temperature susceptibility measurements were carried out in the temperature range 2–300 K with an applied magnetic field of 0.1 T on ground polycrystalline samples of compounds **1** and **2** (with masses of 20.44 and 5.68 mg, respectively), using a Quantum Design MPMS XL-5 SQUID magnetometer. The susceptibility data were corrected for the sample holders previously measured under the same conditions and for the diamagnetic contributions of the sample using tables of Pascal's constants.[15]

ESI-mass spectra were obtained with a Waters Micromass ZQ spectrometer in the positive ion mode. The cone voltage was set to 10 V and the extractor voltage to 5 V, in order to avoid fragmentation. In all cases, well-resolved isotopic patterns consisting of mono-isotopic peaks separated by $1/z$ Da were obtained.

Elemental analysis (C, N, H) of bulk samples was performed by microanalytical procedures using an EA 1110 CHNS-O elemental analyzer from CE instruments. The Cu : F and Cu : Cl ratios of the bulk samples were estimated by electron probe microanalysis (EPMA) performed with a Philips SEM XL30 equipped with an EDAX DX-4 microprobe.

The phase purity of polycrystalline samples **1** and **2** was established by XRPD. Polycrystalline samples were lightly ground in an agate pestle and mortar and placed into 0.7 mm borosilicate capillaries. Data were collected at room temperature in the 2θ range of 2–30° on a Empyrean PANalytical powder diffractometer, using Cu Kα radiation ($\lambda = 1.54177$ Å). In both cases, the powder diffraction pattern of the bulk sample was consistent with the pattern calculated from single-crystal data (see Fig. S1 and S2†).

Thermogravimetric analysis of **2** was carried out with a Mettler Toledo TGA/SDTA 851 apparatus in the 25–1000 °C temperature range under a 5 °C min^{-1} scan rate and an air flow of 30 mL min^{-1}.

UV-visible spectra were recorded for **1** and **2** on a Perkin-Elmer Lambda 1050 Wideband UV-Vis-NIR spectrophotometer in $CHCl_3$ solutions in the range 300 to 850 nm. To follow the inter-conversion, compound **1** (or **2**) was dissolved in 160 μL of CH_3OH ($CHCl_3$ for **2**) and successive 10 μL aliquots of $CHCl_3$ (CH_3OH for **2**) were added to the solution.

Results and discussion

Synthesis

As a ligand we used the pyrazole derivative 3,5-dimethylpyrazolate (3,5-Me$_2$pz$^-$). In its anionic form this ligand has shown

a marked tendency to form polynuclear Cu^{II} complexes containing Cu–N–N–Cu bridges (see Scheme 1), leading to nuclearities ranging from two[16–23] to twelve,[24,25] including three,[26,27] five,[18] eight[28] and eleven,[18] although to date, none with six.

The reaction of this ligand in chloroform/methanol or methanol with $Cu(BF_4)_2 \cdot H_2O$ in a basic medium gives a green solution that after slow diffusion of diethyl ether yields bluish-green single crystals of **1**. Addition of water to a green chloroform solution of **1** yields a purple organic phase that, upon slow diffusion of acetonitrile, affords single crystals of **2**.

X-ray crystal structures

Complex **1** contains six Cu^{II} centres distributed in two eclipsed, almost parallel isosceles triangles (Cu1Cu1′Cu2 and Cu3Cu3′Cu4, see Fig. 1), forming an uncommon trigonal prismatic geometry. This trigonal prism has a central F^- ligand shared by the six Cu^{II} centres, resulting in a sandglass-shaped complex with a μ_6-F^- bridge (Fig. 1). The Cu–Cu distances inside the triangles (2.833(1)–3.112(1) Å) are slightly shorter than those between the triangles (3.056(2)–3.382(2) Å). Each copper atom presents a distorted square pyramidal geometry with Addison parameters of 0.14, 0.04, 0.13 and 0.12 for Cu1–Cu4, respectively.[29] In each case, the basal plane is formed by two nitrogen atoms from two 3,5-Me_2pz^- ligands and by two oxygen atoms from a μ_3-OCH_3^- and a μ_2-OCH_3^- ligand. The axial ligand is in all cases the fluorine atom (F1) of the central μ_6-F^- bridge, located between the two copper triangles (Fig. 1).

Both isosceles triangles are similar and present a symmetry plane that passes through Cu2 and Cu4 and intersects the Cu1–Cu1′ and Cu3–Cu3′ edges. Besides the common μ_6-F^- bridge, both triangles are also connected by: (i) a μ_2-OH^- bridge (O2) connecting Cu2 with Cu4, with a Cu2–O2–Cu4 bond angle of 103.0(3)°; and (ii) two 3,5-Me_2pz^- ligands connecting Cu1 with Cu3 and Cu1′ with Cu3′ through a Cu–N–N–Cu bridge. Each triangle has a μ_3-OCH_3^- bridge connecting the three Cu atoms. The corresponding μ_3-O atoms (O31 and O32) are located 0.97 Å and 0.99 Å out of the Cu2Cu1Cu1′ and Cu4Cu3Cu3′ planes, respectively. Besides these μ_3-OCH_3^- bridges, connectivity inside each triangle is also provided by (i) a μ_2-CH_3O^- bridge connecting the two equivalent copper atoms (Cu1 with Cu1′ and Cu3 with Cu3′); and (ii) two μ_2-3,5-Me_2pz^- bridges connecting the non-equivalent copper atoms (Cu2 with Cu1 and Cu1′ in one triangle and Cu4 with Cu3 and Cu3′ in the other). As observed in the μ_3-OCH_3^- bridges, the oxygen atoms of the μ_2-OCH_3^- bridges (O33 and O34) are not co-planar with the corresponding triangles: O33 is located 0.158 Å above the Cu2Cu1Cu1′ plane and O34 is located 0.276 Å below the Cu4Cu3Cu3′ plane, leading to dihedral angles of 7.0° (Cu2Cu1Cu1′O33) and 11.6°
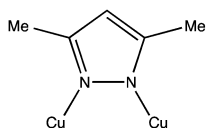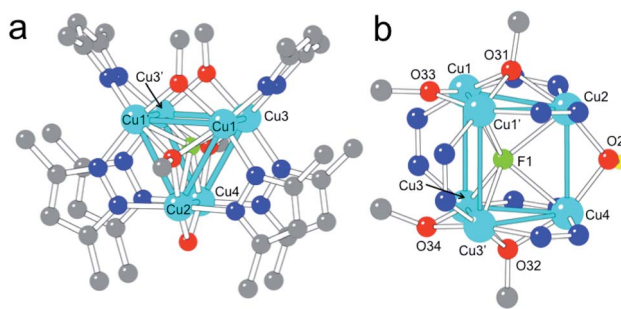

Fig. 1 (a) Top view of complex **1** showing the 3,5-Me_2pz^- ligands and the π–π overlap of the pyrazolate rings. (b) Central portion of the structure of the same complex showing the atom labelling of Cu, F and O atoms and the coordination environments of the six Cu^{II} centres. (H atoms have been omitted for clarity except that of the OH group). Colour code: Cu = cyan, O = red, N = dark blue, C = grey, H = yellow, F = green.

(Cu4Cu3Cu3′O34). In summary, complex **1** has six Cu^{II} ions in an uncommon trigonal prismatic geometry connected by a central μ_6-F^- bridge. The connectivity of the cluster is completed by a μ_2-OH^- bridge (O2), two μ_2-OCH_3^- bridges (O33 and O34), two μ_3-OCH_3^- bridges (O31 and O32) and six μ_2-3,5-Me_2pz^- bridges, leading to a total anionic charge of -12 that compensates the charge of the six Cu^{II} ions.

Although the presence of a central μ_6-F^- bridge is not straightforward to observe from the X-ray crystal analysis (it could also be a OH^- or even a O^{2-} bridge), we have confirmed the presence of fluorine in compound **1** through electron probe microanalysis (EPMA), which indicates the presence of one F atom per Cu_6 cluster. Note that, although in the synthetic procedure there is no addition of F^-, the partial dissociation of the BF_4^- counter-anion of the precursor $Cu(BF_4)_2$ salt can release F^- anions, as has been previously reported.[30–37] Once the nature of the central atom is established, the O2 bridge has to be assigned to a OH^- group in order to maintain the balance of charge (if this was also a F^- atom, it would imply a Cu : F ratio of 3 instead of 6).

The presence of a μ_6-F^- bridge is not unprecedented and has been reported in a family of three compounds, in which the F^- ion is surrounded by six Ag^+ ions in a octahedral environment.[38,39] Compound **1** is, however, the first example of a μ_6-F^- bridge with a trigonal prismatic geometry. Notice also that the presence of any μ_6-X bridge surrounded by six Cu^{II} ions is very unusual in coordination chemistry. Thus, only four μ_6-Cl^-,[40–42] three μ_6-V,[43–45] two μ_6-S,[46,47] one μ_6-Br^-,[48] one μ_6-I,[49] one μ_6-O^{2-},[50] and one μ_6-H^{51} have been reported to date. Among these 13 examples, there is only one (the μ_6-Cl^- complex $[Cu_6(\mu_6Cl)(\mu_3OCH_3)_2(\mu_2pyrazolate)_9]$,[42]) in which the six copper atoms present a trigonal prismatic geometry as in **1**. In summary, **1** is the first copper complex with a μ_6-F^- bridge, and the first example for any metal with trigonal prismatic geometry around a μ_6-F atom.

Besides the central μ_6-F^- bridge, the trigonal prismatic arrangement of the six Cu^{II} ions is stabilized by two μ_2-3,5-Me_2pz^- bridges connecting Cu1–Cu3 and Cu1′-Cu3′, a μ_2-OH^- bridge connecting Cu2 and Cu4 and by two quite strong π–π interactions between the rings of the μ_2-Me_2pz^- bridges,

Scheme 1 The 3,5-dimethylpyrazolate (3,5-Me_2pz^-) ligand connecting two copper atoms, as found in complexes **1** and **2**.

forming two of the three edges of the triangles (the distance between the average planes of the 3,5-Me$_2$pz$^-$ ligands is 3.73 Å, Fig. 1a).[52] Note that an octahedral arrangement of the six Cu^{II} ions would weaken all these interactions except the central μ$_6$-F$^-$ one.

Complex **2** also contains a Cu$_6$ cluster, although with a regular planar hexagonal arrangement of the six equivalent Cu^{II} ions (Fig. 2a). This hexagonal wheel-like structure is packed in the solid state forming hexagonal channels along the c axis (Fig. 3) with an internal diameter of 6.355 Å (measured as the Cu–Cu distance along the diagonal), and a free pore diameter of *ca.* 3.5 Å. The Cu^{II} ions present a square planar geometry with two *trans* N atoms (N1 and N2) from two μ$_2$-3,5-Me$_2$pz$^-$ ligands, and two *trans* oxygen atoms (O1) from two μ$_2$-OH$^-$ bridges (Fig. 2b). Note that the channel structure of compound **2** suggests the possible inclusion of guest molecules, as will be discussed below.

Each pair of two consecutive Cu^{II} ions are connected by two different bridges, alternating on one or the other side of the ring: (i) a –N–N– bridge from a μ$_2$-3,5-Me$_2$pz$^-$ bridge and (ii) a μ$_2$-OH$^-$ bridge with a Cu1–O1–Cu1 bond angle of 110.18° (Fig. 2b). The Cu–O and the Cu–N bond lengths are all similar (in the range 1.936–1.960 Å). The Cu–Cu distance along the side of the hexagon is 3.178(2) Å.

The hexagonal ring in **2** resembles the numerous examples of metalla-crown complexes, whose very interesting host–guest interactions and potentialities have been reviewed by Pecoraro *et al.*,[53] although in **2** the connecting unit between two oxygen atoms is a Cu^{II} centre instead of a –M–N– bridging group. In addition, an interesting feature of this structure is the presence of a CHCl$_3$ and a CH$_3$CN molecule inside the Cu$_6$ ring (confirmed by thermo-gravimetric analysis, Fig. S3†). Both molecules present a positional disorder over two related positions with occupancy factors of 1/2. The CHCl$_3$ molecules are always located above (or below) the Cu$_6$ plane with the three Cl
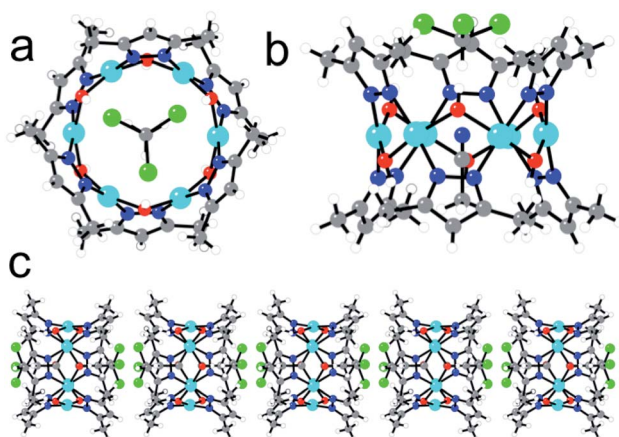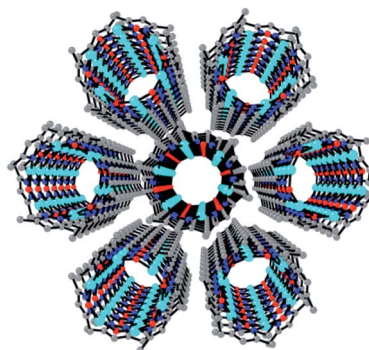

Fig. 3 Perspective view along the c direction of the hexagonal channels in the structure of **2**. H and solvent atoms are omitted for clarity. Colour code: Cu = cyan, O = red, N = dark blue, C = grey.

atoms pointing out of the ring and the H atom pointing towards the centre of the ring (Fig. 2c). The CH$_3$CN molecules are in the centre of the molecule with the N atom located in the Cu$_6$ plane and the two C atoms pointing to one or the other side, depending on the position of the CHCl$_3$ molecule (Fig. 2). Since single crystals of compound **2** are only obtained from a CHCl$_3$ solution after slow diffusion of CH$_3$CN, it seems that both solvent molecules play an important templating role in the crystallization of the Cu$_6$ metalla-cycle.

This kind of Cu$_6$ ring structure with double bridges (O and –N–N–) has already been described in a few cases,[54–59] although they are all charged or contain an ion (mainly Cl$^-$, Br$^-$, I$^-$ or NO$_2^-$). Interestingly, in **2** the Cu$_6$ ring structure is charge-balanced and, therefore, **2** is the first example of a neutral Cu$_6$ ring of this type without any counter-ion inside. This fact explains the eclipsed packing of the rings leading to an unprecedented tubular structure with hexagonal channels that can be evacuated (Fig. 3).

One-dimensional pores are highly interesting, since their tubular topology can afford a high adsorption capacity with size selectivity and one dimensional diffusion properties. The presence of the solvent molecules in the Cu$_6$ channels prevents the crystal from exhibiting a well-defined nano-porous structure, as occurs in other metalla-cycles. Still, as these solvent molecules are neutral, they can be partially removed upon heating in a single-crystal-to-single-crystal process, without loss of crystallinity. This affords a porous material (15–17% of the unit cell volume) with a pore diameter of *ca.* 3.55 Å, slightly larger than the kinetic CO$_2$ diameter (3.30 Å). Indeed, preliminary gas sorption studies show that CO$_2$ molecules can partially enter into the one-dimensional pores with an uptake of up to *ca.* 30% v/v of CO$_2$ in the hexagonal channels of a de-solvated sample of compound **2** with a CO$_2$ pressure of *ca.* 1 atm (Fig. S4†).

Stability in solution of the Cu$_6$ compounds

A green CHCl$_3$ solution of compound **1** presents an ESI-mass spectrum with four main signals centred at m/z = 1069.23, 1049.13, 1021.25 and 1003.18 Da in the positive region (Fig. 4). These four signals can be attributed to hexanuclear Cu^{II}

Fig. 2 (a) Top view of the Cu$_6$ wheel showing the CHCl$_3$ molecule and the three H atoms of the CH$_3$CN molecule located in the central channel. (b) Side view of the same molecule showing one of the two possible locations of the CHCl$_3$ and CH$_3$CN molecules. (c) Side view of the hexagonal channels showing the two possible locations of the CHCl$_3$ and CH$_3$CN molecules. Colour code: Cu = cyan, O = red, N = dark blue, Cl = green, C = grey, H = white.

complexes with 3,5-Me$_2$pz$^-$ (L) bridges presenting different degrees of hydrolysis and different amounts of O^{2-}, OH$^-$ and CH$_3$O$^-$ bridges: {Cu$_6$(L)$_6$(F)(OH)$_3$(O)(CH$_3$O) $-$ 2e$^-$}$^+$ (m/z = 1069.06), [Cu$_6$(L)$_6$(F)(O)(CH$_3$O)$_2$]$^+$ (m/z = 1049.08), [Cu$_6$(L)$_6$-(F)(O)(OH)$_2$]$^+$ (m/z = 1021.07) and [Cu$_6$(L)$_6$(F)(O)$_2$]$^+$ (m/z = 1003.01), with isotopic patterns matching those observed experimentally (Fig. 4), confirming the presence of the μ$_6$-F$^-$ hexanuclear Cu^{II} complex **1** in solution and its stability.

The ESI-mass spectrum of compound **2** dissolved in a 1 : 1 CHCl$_3$–CH$_3$OH mixture shows three main signals centred at m/z = 1067.17, 1081.18 and 1097.21 Da in the positive region (Fig. 4). These three signals correspond to those expected for an ionized Cu$_6$ wheel with a partial substitution of one, two or three μ-OH$^-$ bridges by the corresponding μ-OCH$_3^-$ bridges, together with the loss (or gain) of H atoms and electrons (Fig. 4). We can conclude that the {[Cu$_6$(3,5-Me$_2$pz)$_6$(OH$_n$)(OH)$_{5-x}$-(CH$_3$O)$_x$] $-$ ze$^-$}$^+$ monocations with x = 1 and 2 (n/z = 0/2), and x = 3 (n/z = 2/0) with average masses of 1067.07, 1081.10 and 1097.14 Da and with isotopic patterns matching those observed experimentally are present in the solution, showing the stability of the Cu$_6$ wheel and the progressive OH$^-$/CH$_3$O$^-$ ligand exchange.

Conversion from 1 to 2

When a CHCl$_3$ solution of **1** is left to stand in open air, a colour change from green to purple is observed on the surface after a few hours. This colour change is caused by the diffusion of water molecules from the air, and can indeed be promoted by addition of water, yielding a purple solution that, upon slow diffusion of acetonitrile, affords single crystals of **2**. Thus, conversion of **1** into **2** can be achieved in this way. A possible pathway for this conversion is depicted in Fig. 5. The addition of water molecules may cause the hydrolysis of the easily accessible μ$_2$-OH$^-$ (O2) and the two μ$_3$-OCH$_3^-$ bridges (O32 and O33 in Fig. 1). This kind of process has already been observed in other similar trinuclear pyrazolato-Cu^{II} complexes with alkoxido bridges.[60] Once hydrolysed, these three bridges are released, allowing the unfolding of the Cu$_6$ trigonal prism into a planar Cu$_6$ hexagon by a simple rotation of 90° of both triangles around the Cu3–Cu3′ and Cu1–Cu1′ edges (Fig. 5). Note that this mechanism does not imply cleavage nor formation of any Cu–N bond during the process, since the number and connectivity of the μ$_2$-3,5-Me$_2$pz$^-$ ligands remains the same in both compounds. The transformation of the Cu$_6$ arrangement is clearly followed by the change of colour of the solution (from green to purple). Addition of CH$_3$CN to the purple solution containing the wheels permits the crystallization of **2**.

In order to check if the conversion of **1** into **2** is reversible, we have followed the changes in colour of a solution containing these species upon changing the solvent mixture. We have found that by adding methanol to the purple solution of **2**, the colour changes to a green colour very close to that of the original solution of **1**, but not identical, indicating that complex **2** is transformed into a complex very similar to **1** under these conditions. These colour changes have been monitored in a more precise way by recording UV-vis absorption spectra. In the visible region **1** shows a broad double maximum in the range of 550 to 600 nm, while **2** shows a maximum at 528 nm (ε = 512) and a shoulder at *ca.* 610 nm (Fig. 6).

The spectra of a solution of **2** in 160 μL of CHCl$_3$ with different added aliquots of CH$_3$OH (10 μL to 160 μL) are shown in Fig. 7. These show that the maximum at 528 nm decreases in intensity upon addition of CH$_3$OH, and eventually disappears. At the same time a new maximum starts to appear when 60 μL of CH$_3$OH is added. This new maximum increases in intensity and moves to lower energies to reach a constant value of 630 nm when 160 μL has been added. This maximum is similar, although not identical, to that observed in the spectrum of **1** in a solution of CHCl$_3$ and 160 μL of CH$_3$OH (Fig. S5†), and indicates that compound **2** converts into a compound closely related to **1**. Two isosbestic points at approximately 473 and 525 nm are also observed, indicating that an equilibrium between both species is established when small quantities of CH$_3$OH are added to an initial CHCl$_3$ solution (Fig. 7).

Finally, it should be mentioned that when 10 μL of H$_2$O was added to a solution of **1** in CHCl$_3$ plus 160 μL of CH$_3$OH, the colour of the solution changed from green to blueish-purple, indicating that **2** is formed. When larger amounts of water were added, the visible spectra of these solutions remained practically identical to that of a solution of **2** in these solvents (Fig. S6†), until the addition of 30 μL of H$_2$O; at that point the organic solution formed a suspension.
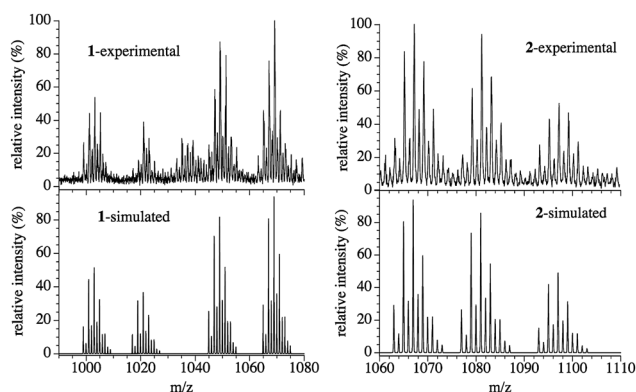

Fig. 4 Experimental (top) and simulated (bottom) ESI-mass spectra of compounds **1** (left) and **2** (right).
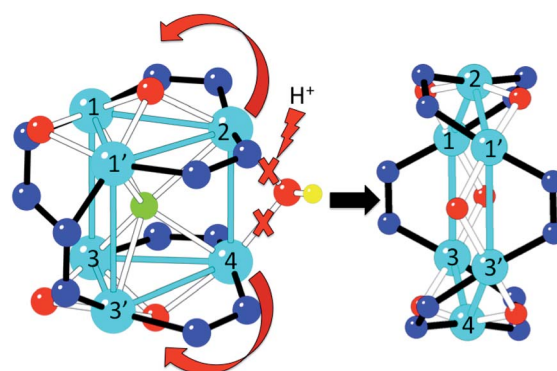

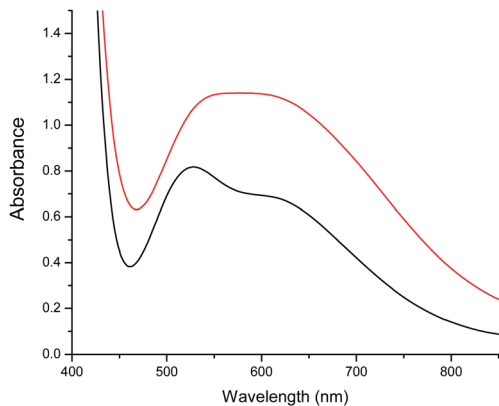**Fig. 5** Proposed mechanism for the transformation of **1** into **2**.
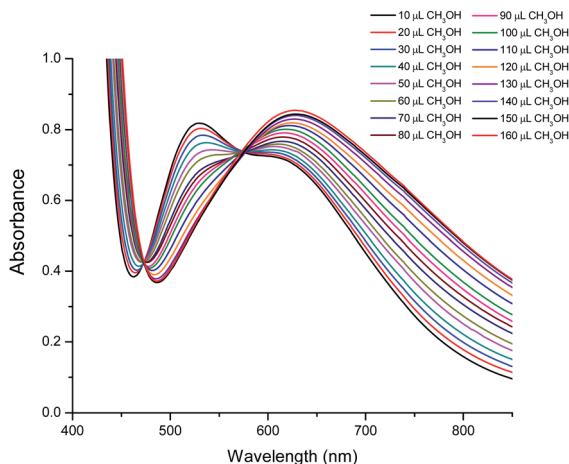
Fig. 6 Absorption spectra of **1** (red) and **2** (black) in CHCl₃.

Fig. 7 Visible spectra of compound **2** in CHCl₃ with different quantities of CH₃OH, showing the transformation of **2** into a complex similar to **1**.

All these transformations have also been followed with ESI-mass spectroscopy. The addition of water to a green solution containing **1** leads to the formation of a purple solution whose ESI-mass spectrum is the same as a solution of **2** in CHCl₃ (Fig. 4), which clearly demonstrates the transformation of **1** into **2**. Finally, the addition of an excess of CH₃OH to the purple solution of **2** results in a green solution that contains trimeric Cu^{II} units connected by 3,5-Me₂pz⁻ (L) ligands with a presumed structure very similar to that present in **1**. The ESI-mass spectrum of this resulting green solution presents three main signals centred at m/z = 666.24, 602.42 and 571.23 Da (Fig. S8†), corresponding to Cu^{II} trimers with different hydrolysis degrees and different amounts of CH₃OH and CH₃O⁻ bridges: {[Cu₃(L)₃(CH₃OH)₄(CH₃O)₂]}⁺ (m/z = 666.24), {[Cu₃(L)₃-(CH₃OH)₂(CH₃O)₂]}⁺ (m/z = 602.16) and {[Cu₃(L)₃(CH₃OH)₂(CH₃O)]+1e⁻}⁺ (m/z = 571.12). These spectra indicate that **1** transforms into **2**, whereas **2** transforms into a trimeric Cu^{II} cluster very similar to each of the two trimeric species that form compound **1**, although containing only CH₃O⁻ and CH₃OH bridges but no hydroxido or fluoride ones.

A possible explanation of the non-reversibility of the reaction is the lack of F⁻ anions in the medium that could act as μ₆-

bridges. However, even in the presence of an excess of F⁻ (or BF₄⁻), the Cu₆ wheel does not convert back into **1**.

Magnetic properties

These two Cu₆ complexes exhibit strong differences in their magnetic behaviour, which can be correlated with their molecular structures. Thus, for **1** a smooth decrease of the product of the molar magnetic susceptibility and temperature ($\chi_m T$) is observed upon cooling, exhibiting a $\chi_m T$ value of *ca.* 1.9 emu K mol⁻¹ at 300 K, which decreases to reach an intermediate $\chi_m T$ value of 0.7 emu K mol⁻¹ at 10 K, and finally shows a sharp decrease at lower temperatures. In contrast, for **2** this decrease is much sharper, exhibiting a much lower $\chi_m T$ value even at room temperature (0.5 emu K mol⁻¹), which tends to be zero below 50 K (Fig. 8). Qualitatively this difference indicates that in these magnetic clusters the Cu^{II} spins are much more strongly antiferromagnetically coupled in **2** than in **1**. It also indicates that for **2**, the antiferromagnetic spin state $S = 0$ is the ground state, being well separated in energy from the first excited spin states, while for **1** the spin states $S = 0$ and $S = 1$ must be quasi-degenerate to explain the tendency of $\chi_m T$ to reach an intermediate value (*ca.* 0.7 emu K mol⁻¹) at low temperatures. In other words, in this last cluster the behaviour is dominated by two antiferromagnetic triangles, each having a ground spin state of $S = 1/2$. In the frame of this model, the sharp decrease in $\chi_m T$ observed in the low temperature limit should indicate the presence of weaker antiferromagnetic coupling between these two triangular units.

In order to give a quantitative explanation, these magnetic data have been fitted to spin models that take into account the structural features of these Cu₆ magnetic clusters using the package MAGPACK.[61,62] In these models, the Hamiltonian describing the exchange interaction between sites i and j is written as $-JS_iS_j$. Structurally, **1** possesses two isosceles triangles connected through three different bridges (two μ₂-3,5-Me₂pz⁻, one μ₂-OH⁻ and the central μ₆-F⁻, Fig. 1). This low symmetry leads to a complex exchange network formed by two exchange interactions inside the triangles and two different exchange interactions connecting the two triangles (Scheme 2). Taking into
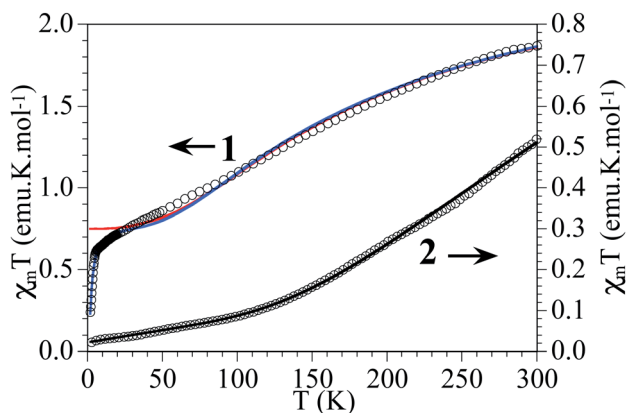

Fig. 8 Thermal variation of $\chi_m T$ per Cu₆ unit in **1** and **2**. Solid lines are the best fit to the models (see text).

account the above remarks, we first extracted the exchange interactions within the triangles (J_1 and J_2) by fitting the magnetic data in the temperature range 30 K < T < 300 K to an isolated triangle (*i.e.*, J_3 and J_4 have been fixed to 0). The resulting curve is plotted as a red line in Fig. 8 (extrapolated down to 2 K). In a second step, to fit the low temperature behaviour, we fixed J_1 and J_2 to these values, while allowing J_3 and J_4 to vary. As these two parameters have been found to be strongly correlated, we have performed DFT calculations to estimate J_3 (ESI†). The obtained value for J_3 (-22 cm^{-1}) agrees well with the calculated values for two similar pyrazolato bridges in two closely related Cu$_6$ trigonal prisms.[42,63] Note that this J_3 exchange pathway involves a pyrazolato Cu–N–N–Cu bridge, and that this bridge gives rise to antiferromagnetic coupling when the pyrazolate bridge connects two basal positions, but the magnitude strongly depends on the angle formed by the two basal planes. Thus, when the two basal planes are coplanar, the antiferromagnetic coupling is strong, but when this angle decreases, the magnetic coupling significantly decreases.[64–66] In **1** the two basal planes are far from being coplanar, forming an angle of 58.6° and, therefore it is expected to lead to a weak antiferromagnetic coupling, in agreement with the calculated J_3 value (-22 cm^{-1}). Fixing this value in the fitting procedure, the final set of exchange parameters is $J_1 = -94$ cm^{-1}; $J_2 = -131$ cm^{-1}, $J_3 = -22$ cm^{-1} and $J_4 = -4$ cm^{-1} (the fit with these values corresponds to the blue line in Fig. 8). As can be seen in Scheme 2, J_1 (-94 cm^{-1}) corresponds to a double bridge formed by a pyrazolate (–N–N–) and a methoxido bridge. This kind of bridge is well known to produce moderate to strong antiferromagnetic (AF) couplings (in the range *ca.* -160 to -550 cm^{-1}),[16] with stronger AF coupling as the Cu–O–Cu angle increases. In **1** this angle is very small (102.1(2)°) compared with most of the reported examples (with angles in the range *ca.* 120–130° and, accordingly, this AF coupling is weaker than those observed in the other examples). The second coupling constant, J_2, (-131 cm^{-1}) corresponds to a double methoxido bridge (Scheme 2 and Fig. 1). The coupling through this kind of bridge is mainly determined by the Cu–O–Cu bond angle (α) and the angle formed by the C–O bond with the Cu$_2$O$_2$ central unit (τ) when this central unit is planar.[67,68] These correlations establish that when $\tau = 0$, the coupling is AF for α angles above *ca.* 88.5°, but for $\tau = 40$° the crossing point shifts to *ca.* 94.5°. In **1** the Cu–O–Cu angles are 90.8(2)° (Cu1–O31–Cu1′) and 96.5(3)° (Cu1–O33–Cu1′) and the corresponding τ angles are *ca.* 40° and *ca.* 10°, respectively (the lack of planarity of the central Cu$_2$O$_2$ unit precludes a precise

calculation of τ). These values suggest that the Cu1–O31–Cu1′ exchange pathway should be weak and ferromagnetic, whereas the Cu1–O33–Cu1′ pathway should be stronger and AF, resulting in the observed moderate AF coupling for this double methoxido bridge. Note also that the lack of planarity in the basal planes of Cu1 and Cu1′ or Cu3 and Cu3′ (the dihedral angles between their average planes are 135.5° and 133.6°, respectively) is expected to further decrease the resulting magnetic exchange. Finally, J_4 (-4 cm^{-1}) corresponds to a hydroxido bridge with a Cu–O–Cu bond angle of 103.0(3)°. Note that previous magneto-structural correlations in this kind of bridge[67,68] indicate that, in general, this coupling should be strongly antiferromagnetic. The much weaker coupling observed for this bridge in **1** has to be attributed to the fact that the basal planes of the two Cu^{II} ions are almost orthogonal (the dihedral angle is 94.9°), resulting in an almost null orbital overlap.

Compound **2** at room temperature shows a $\chi_m T$ value of *ca.* 0.5 emu K mol^{-1} per Cu$_6$ ring, well below that expected for six independent Cu^{II} ions. When the temperature is decreased, $\chi_m T$ shows a continuous decrease to reach a value of *ca.* 0.02 emu K mol^{-1} at 2 K (Fig. 8). This behaviour indicates that compound **2** shows a strong antiferromagnetic coupling inside the Cu$_6$ cluster with a small contribution from paramagnetic impurities. The isothermal magnetization at 2 K (Fig. S9†) confirms this behaviour. In compound **2** the model used to fit the magnetic properties is much more simple, since the six coupling constants inside the Cu$_6$ ring are identical, and therefore we only need to consider one exchange constant. The fitting was done by the same methodology used for **1**.[61,62] With this simple model the magnetic properties of compound **2** can be very well reproduced over the whole temperature range, including a paramagnetic monomeric Cu^{II} impurity (ρ) with the following parameters: $J_1 = -454$ cm^{-1} and $\rho = 0.23\%$, with a fixed value of $g = 2.1$ (solid line in Fig. 8).

The value found for the coupling constant in compound **2** is close to those found in other similar Cu complexes with the same kind of double bridge and similar structural parameters.[16]

Furthermore, from previous magneto-structural correlations in Cu^{II} complexes with hydroxido bridges,[67,68] in compound **2** we can estimate a J value of *ca.* -450 cm^{-1}, in very good agreement with the experimental value.

Conclusions

In this work we present the structural and magnetic characterization of two new hexanuclear Cu^{II} complexes: [Cu$_6$(μ_6F)(μ_2OH)(μ_3OCH$_3$)$_2$(μ_2OCH$_3$)$_2$(3,5-Me$_2$pz)$_6$] (**1**) and [Cu$_6$(μ_2OH)$_6$(3,5-Me$_2$pz)$_6$]·CH$_3$CN·CHCl$_3$ (**2**), and a possible mechanism of the transformation of **1** into **2**. Complex **1** exhibits a sandglass-like structure, and represents the first copper complex with a μ_6-F$^-$ bridge and the first metallic complex with trigonal prismatic geometry around a μ_6-F atom. Compound **2** is formed from a neutral and soluble wheel-like Cu$_6$ complex, which packs in the solid state to give a tubular structure that contains CH$_3$CN and CHCl$_3$ molecules in the hexagonal channels formed by the eclipsed packing of the Cu$_6$ rings. These solvent molecules can be removed and partially
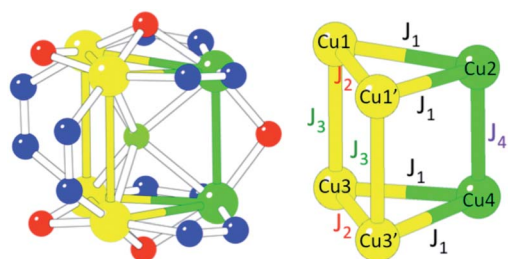
Scheme 2 Magnetic exchange scheme and coupling constants used to fit the magnetic properties of the Cu$_6$ cluster in **1**.

exchanged with CO_2 since the removal of the solvent molecules does not alter the crystal structure of **2**. Visible and mass spectra confirm the conversion of **1** into **2** by simply changing the solvent conditions. The stability of the Cu_6 wheel in solution opens up the possibility of preparing thin films of this entity with a mono-disperse porous tubular structure by using different solution-based techniques. These two compounds exhibit very different magnetic behaviours, in agreement with their structural features. Thus, the spin structure of **1** shows a ground state formed of quasi-degenerate $S = 0$ and $S = 1$ spin levels, as it is dominated by a spin frustration effect within the two antiferromagnetic triangles. In turn, **2** shows an antiferromagnetic ground spin state $S = 0$, which is well separated in energy from the first excited $S = 1$ spin state (by more than 62 cm^{-1}), as a consequence of the very strong antiferromagnetic Cu–Cu interactions and of the hexagonal topology of the exchange network.

Acknowledgements

References

1 M. Fu, I. Issac, D. Fenske and O. Fuhr, *Angew. Chem., Int. Ed.*, 2010, **49**, 6899–6903.

2 B. Murphy and B. Hathaway, *Coord. Chem. Rev.*, 2003, **243**, 237–262.

3 A. M. Kirillov, M. V. Kirillova and A. J. L. Pombeiro, *Coord. Chem. Rev.*, 2012, **256**, 2741–2759, DOI: 10.1016/j.ccr.2012.07.022.

4 E. I. Solomon, U. M. Sundaram and T. E. Machonkin, *Chem. Rev.*, 1996, **96**, 2563–2606.

5 D. Desbouis, I. P. Troitsky, M. J. Belousoff, L. Spiccia and B. Graham, *Coord. Chem. Rev.*, 2012, **256**, 897–937.

6 I. Blain, P. Slama, M. Giorgi, T. Tron and M. Réglier, *Rev. Mol. Biotechnol.*, 2002, **90**, 95–112.

7 M. C. Feiters, *Comments Inorg. Chem.*, 1990, **11**, 131–174.

8 V. Wing-Wah Yam, K. Kam-Wing Lo, W. Kit-Mai Fung and C. Wang, *Coord. Chem. Rev.*, 1998, **171**, 17–41.

9 G. Givaja, P. Amo-Ochoa, C. J. Gómez-García and F. Zamora, *Chem. Soc. Rev.*, 2012, **41**, 115–147.

10 O. Kahn, *Molecular Magnetism*, VCH Publishers, USA, 1993.

11 E. Coronado, M. Giménez-Marqués, G. Mínguez Espallargas and L. Brammer, *Nat. Commun.*, 2012, **3**, 828.

12 E. Coronado and G. Minguez Espallargas, *Chem. Soc. Rev.*, 2013, **42**, 1525–1539.

13 G. M. Sheldrick, *Acta Crystallogr., Sect. A: Found. Crystallogr.*, 2008, **64**, 112–122.

14 A. Spek, *J. Appl. Crystallogr.*, 2003, **36**, 7–13.

15 G. A. Bain and J. F. Berry, *J. Chem. Educ.*, 2008, **85**, 532–536.

16 Y. Elerman, H. Kara and A. Elmali, *Z. Naturforsch., A: Phys. Sci.*, 2003, **58**, 363–372.

17 G. A. Ardizzoia, M. A. Angaroni, G. La Monica, N. Masciocchi and M. Moret, *J. Chem. Soc., Dalton Trans.*, 1990, 2277–2281.

18 T. O. Denisova, E. V. Amel'chenkova, I. V. Pruss, Z. V. Dobrokhotova, O. P. Fialkovskii and S. E. Nefedov, *Russ. J. Inorg. Chem.*, 2006, **51**, 1020–1064.

19 G. Mezei and R. G. Raptis, *Inorg. Chim. Acta*, 2004, **357**, 3279–3288.

20 Y. Elerman and A. Elmali, *Z. Naturforsch., B: J. Chem. Sci.*, 2001, **56**, 970–974.

21 Y. Elerman, H. Kara and A. Elmali, *Z. Naturforsch., B: J. Chem. Sci.*, 2001, **56**, 1129–1137.

22 H. Kara, Y. Elerman and K. Prout, *Z. Naturforsch., B: J. Chem. Sci.*, 2001, **56**, 719–727.

23 H. Kara, Y. Elerman and K. Prout, *Z. Naturforsch., B: J. Chem. Sci.*, 2000, **55**, 796–802.

24 V. Chandrasekhar, L. Nagarajan, R. Clerac, S. Ghosh, T. Senapati and S. Verma, *Inorg. Chem.*, 2008, **47**, 5347–5354.

25 V. Chandrasekhar and S. Kingsley, *Angew. Chem., Int. Ed.*, 2000, **39**, 2320–2322.

26 J. He, Y. Yin, T. Wu, D. Li and X. Huang, *Chem. Commun.*, 2006, 2845–2847.

27 M. K. Ehlert, S. J. Rettig, A. Storr, R. C. Thompson and J. Trotter, *Can. J. Chem.*, 1990, **68**, 1444–1449.

28 G. A. Ardizzoia, M. A. Angaroni, G. La Monica, F. Cariati, S. Cenini, M. Moret and N. Masciocchi, *Inorg. Chem.*, 1991, **30**, 4347–4353.

29 A. W. Addison, T. N. Rao, J. Reedijk, J. van Rijn and G. C. Verschoor, *J. Chem. Soc., Dalton Trans.*, 1984, 1349–1356.

30 J. A. Carroll, R. E. Cobbledick, F. W. B. Einstein, N. Farrell, D. Sutton and P. L. Vogel, *Inorg. Chem.*, 1977, **16**, 2462–2469.

31 M. Hidai, T. Kodama, M. Sato, M. Harakawa and Y. Uchida, *Inorg. Chem.*, 1976, **15**, 2694–2697.

32 P. B. Hitchcock, M. F. Lappert and R. G. Taylor, *J. Chem. Soc., Chem. Commun.*, 1984, 1082–1084.

33 F. J. Rietmeijer, R. A. G. De Graaff and J. Reedijk, *Inorg. Chem.*, 1984, **23**, 151–156.

34 R. H. Crabtree, G. G. Hlatky and E. M. Holt, *J. Am. Chem. Soc.*, 1983, **105**, 7302–7306.

35 S. Herold and S. J. Lippard, *Inorg. Chem.*, 1997, **36**, 50–58.

36 Y. Zang, H. G. Jang, Y. Chiou, M. P. Hendrich and L. Que, Jr, *Inorg. Chim. Acta*, 1993, **213**, 41–48.

37 V. Terruzzi, U. Comin, F. De Grazia, G. L. Toti, A. Zambelli, S. Beretta and G. Minoli, *Gastrointest. Endosc.*, 2000, **51**, 23–27.

38 Q. Wang, G. Guo and T. C. W. Mak, *Polyhedron*, 2003, **22**, 217–223.

39 Q. Wang and T. C. W. Mak, *Chem. Commun.*, 2000, 1435–1436.

40 E. V. Lider, E. V. Peresypkina, A. I. Smolentsev, V. N. Elokhina, T. I. Yaroshenko, A. V. Virovets, V. N. Ikorskii and L. G. Lavrenova, *Polyhedron*, 2007, **26**, 1612–1618.

41 E. V. Govor, A. B. Lysenko, D. Quinonero, E. B. Rusanov, A. N. Chernega, J. Moellmer, R. Staudt, H. Krautscheid, A. Frontera and K. V. Domasevitch, *Chem. Commun.*, 2011, **47**, 1764–1766.

42 A. Kamiyama, T. Kajiwara and T. Ito, *Chem. Lett.*, 2002, 980–981.

43 D. G. Chen, H. H. Zhang and X. F. Yu, *Chin. J. Struct. Chem.*, 2003, **22**, 591–594.

44 C. D. Scattergood, P. G. Bonney, J. M. Slater, C. D. Garner and W. Clegg, *J. Chem. Soc., Chem. Commun.*, 1987, 1749–1750.

45 F. Zheng, H. H. Zhang, R. P. Zhou, Y. S. Wu, X. F. Yu and J. S. Huang, *Chin. J. Struct. Chem.*, 1997, **16**, 392.

46 R. E. Marsh, *Acta Crystallogr., Sect. B: Struct. Sci.*, 1997, **53**, 317–322.

47 P. Lin, X. Wu, L. Chen, L. Wu and W. Du, *Polyhedron*, 2000, **19**, 2189–2193.

48 Z. Wei, H. Li, M. Cheng, X. Tang, Y. Chen, Y. Zhang and J. Lang, *Inorg. Chem.*, 2009, **48**, 2808–2817.

49 E. Jalilian and S. Lidin, *CrystEngComm*, 2011, **13**, 5730–5736.

50 B. Li, J. Zhao, S. Zheng and G. Yang, *Inorg. Chem.*, 2009, **48**, 8294–8303.

51 R. D. Kohn, Z. Pan, M. F. Mahon and G. Kociok-Kohn, *Chem. Commun.*, 2003, 1272–1273.

52 C. A. Hunter and J. K. M. Sanders, *J. Am. Chem. Soc.*, 1990, **112**, 5525–5534.

53 G. Mezei, C. M. Zaleski and V. L. Pecoraro, *Chem. Rev.*, 2007, **107**, 4933–5003.

54 J. J. Henkelis, L. F. Jones, M. P. de Miranda, C. A. Kilner and M. A. Halcrow, *Inorg. Chem.*, 2010, **49**, 11127–11132.

55 A. A. Mohamed, A. Burini, R. Galassi, D. Paglialunga, J. Galán-Mascarós, K. R. Dunbar and J. P. Fackler, *Inorg. Chem.*, 2007, **46**, 2348–2349.

56 E. V. Govor, A. B. Lysenko, D. Quinonero, E. B. Rusanov, A. N. Chernega, J. Moellmer, R. Staudt, H. Krautscheid, A. Frontera and K. V. Domasevitch, *Chem. Commun.*, 2011, **47**, 1764–1766.

57 A. A. Mohamed, S. Ricci, A. Burini, R. Galassi, C. Santini, G. M. Chiarella, D. Y. Melgarejo and J. P. Fackler, *Inorg. Chem.*, 2011, **50**, 1014–1020.

58 G. Mezei, P. Baran and R. G. Raptis, *Angew. Chem., Int. Ed.*, 2004, **43**, 574–577.

59 J. Liu, J. Zhuang, X. You and X. Huang, *Chem. Lett.*, 1999, **28**, 651–652.

60 G. Mezei, R. G. Raptis and J. Telser, *Inorg. Chem.*, 2006, **45**, 8841–8843.

61 J. J. Borrás-Almenar, J. M. Clemente-Juan, E. Coronado and B. S. Tsukerblat, *Inorg. Chem.*, 1999, **38**, 6081–6088.

62 J. J. Borrás-Almenar, J. M. Clemente-Juan, E. Coronado and B. S. Tsukerblat, *J. Comput. Chem.*, 2001, **22**, 985–991.

63 E. M. Zueva, M. M. Petrova, R. Herchel, Z. Travnicek, R. G. Raptis, L. Mathivathanan and J. E. McGrady, *Dalton Trans.*, 2009, 5924–5932.

64 S. O. Malinkin, Y. S. Moroz, L. V. Penkova, V. V. Bon, E. Gumienna-Kontecka, V. A. Pavlenko, V. I. Pekhnyo, F. Meyer and I. O. Fritsky, *Polyhedron*, 2012, **37**, 77–84.

65 M. F. Iskander, T. E. Khalil, W. Haase, R. Werner, I. Svoboda and H. Fuess, *Polyhedron*, 2001, **20**, 2787–2798.

66 V. Mishra, F. Lloret and R. Mukherjee, *Eur. J. Inorg. Chem.*, 2007, 2161–2170.

67 E. Ruiz, P. Alemany, S. Alvarez and J. Cano, *Inorg. Chem.*, 1997, **36**, 3683–3688.

68 E. Ruiz, P. Alemany, S. Alvarez and J. Cano, *J. Am. Chem. Soc.*, 1997, **119**, 1297–1303.